

The sizes of coherent band states in semiconductors, derived from the Franz - Keldysh effect

This article has been downloaded from IOPscience. Please scroll down to see the full text article.

1996 J. Phys.: Condens. Matter 8 6779

(<http://iopscience.iop.org/0953-8984/8/36/028>)

View [the table of contents for this issue](#), or go to the [journal homepage](#) for more

Download details:

IP Address: 171.66.16.206

The article was downloaded on 13/05/2010 at 18:39

Please note that [terms and conditions apply](#).

## The sizes of coherent band states in semiconductors, derived from the Franz–Keldysh effect

A Jaeger<sup>†</sup>, G Weiser<sup>†</sup>, P Wiedemann<sup>‡</sup>, I Gyuro<sup>‡</sup> and E Zielinski<sup>‡</sup>

<sup>†</sup> Department of Physics and Centre of Material Sciences, University of Marburg, D-35032 Marburg, Germany

<sup>‡</sup> Alcatel SEL AG, Research Centre, Lorenzstraße 10, D-70435 Stuttgart, Germany

Received 8 May 1996, in final form 24 June 1996

**Abstract.** Electroabsorption spectroscopy with small modulation voltages has been used to study coherent states above the gap of  $\text{In}_{0.53}\text{Ga}_{0.47}\text{As}$ . At very low fields only excitonic effects are observed which disappear in fields as small as  $6 \text{ kV cm}^{-1}$  to become part of the Franz–Keldysh oscillations, the response of the continuum states. Different sets are observed for the three valence bands which vary with field in perfect accordance with theory. The range of oscillations, which at moderate fields extends over 0.5 eV, increases linearly with field and is directly related to the coherence length of the continuum states. The coherence length in the ternary sample is 160 nm, more than twice as large as in a quaternary sample and larger than the value derived from Stark ladder transitions in superlattices.

### 1. Introduction

Epitaxial growth techniques are commonly employed to modify the properties of semiconductors and devices by imposing new boundary conditions onto the electronic states. Quantum wells confine electrons to thin regions by placing the well material between barriers of a wider gap while periodic arrangements of wells and barriers result in superlattices where electrons move freely in bands whose width can be controlled by the growth conditions. Such quantum-size effects require that the artificial boundaries are separated by less than the coherence length of the band states, which is not well known—in contrast to coherent lifetimes which are widely studied by probing nonlinear optical properties with short pulses. Because no obvious method for measuring the coherence length in a semiconductor seems to be available, photocurrent spectra of Stark ladder transitions which appear in superlattices in high electric fields have been used as a substitute. These studies derive coherence lengths of 94 nm and 50 nm at 5 K and 300 K, respectively, for  $\text{GaAs}/\text{Ga}_{1-x}\text{Al}_x\text{As}$  [1] and a similar value (45 nm) for an  $\text{In}_{0.53}\text{Ga}_{0.47}\text{As}/\text{InP}$  superlattice [2]. We demonstrate for an  $\text{In}_{0.53}\text{Ga}_{0.47}\text{As}/\text{InP}$  heterostructure that the Franz–Keldysh effect in homogeneous electric fields provides a convenient tool for measuring the spatial extent of coherent states in bulk semiconductors, also supplementing the information gained from short-pulse experiments. We will also discuss the influence of moderate inhomogeneity of the field due to the space charge from residual doping.

In addition to broadening the absorption edge [3, 4], electric fields induce oscillatory changes of the absorption spectrum above the gap [5–8]. These Franz–Keldysh oscillations are related to the acceleration of an electron by the electric field,  $F$ , which leads to a momentum increasing with time [9]:  $dk/dt = eF/\hbar$ . When  $k$  reaches the edge of the

Brillouin zone at  $\pi/a$ , Bragg reflection occurs and localizes the electron in space, breaking up the band into the Wannier–Stark ladder, discrete levels of which are spaced in energy by  $eFa$  [10]. However, a finite scattering time  $\tau$  limits the wavevector to a maximum value of  $\delta k$  which is usually much smaller than the reciprocal-lattice vector:

$$\delta k = \int_0^\tau \frac{eF}{\hbar} dt. \quad (1)$$

Consequently, Wannier–Stark ladder transitions or, equivalently, Bloch oscillations of an electron [11], have never been observed in bulk material although they have been found in superlattices which have much smaller Brillouin zones [12–14].

The electric field mixes the Bloch states  $\langle k |$  to new eigenstates and alters the transition probability above the gap. The difference between the spectra with and without the field, the electroabsorption spectrum  $\Delta\alpha$ , shows characteristic oscillations above the gap. This  $\Delta\alpha$ -spectrum scales with an electro-optic energy

$$\hbar\Theta = \left( \frac{eF\hbar}{\sqrt{2m^*}} \right)^{2/3} \quad (2)$$

which provides a simple access to the field in the sample [15]. In the case of sufficiently homogeneous fields, the energy range over which the oscillations are observed is limited only by the loss of coherence, which has been modelled by Lorentzian broadening of the spectra or by supplementing the electro-optic energy  $\hbar\Theta$  with an imaginary part [8]. We will show that this range reflects the spatial extent of the coherent states rather than their lifetime.

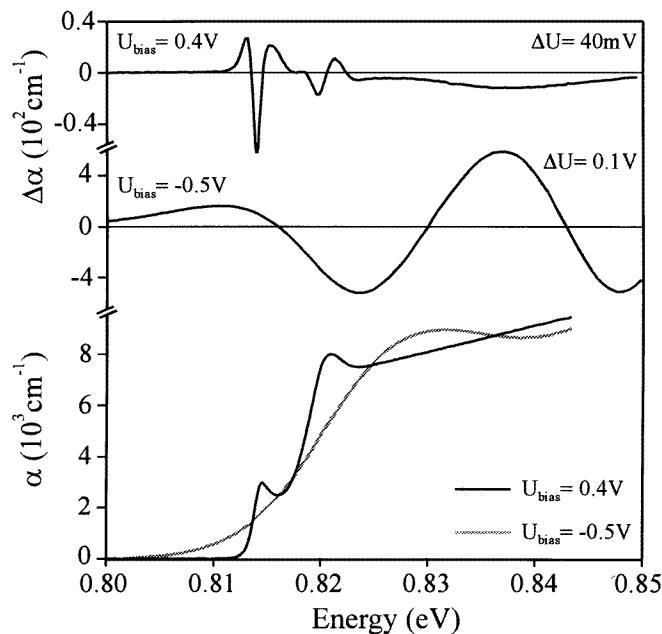


**Figure 1.** A comparison of absorption spectra near the gap for small forward and reverse biases and the change  $\Delta\alpha$  induced by a small ac voltage.

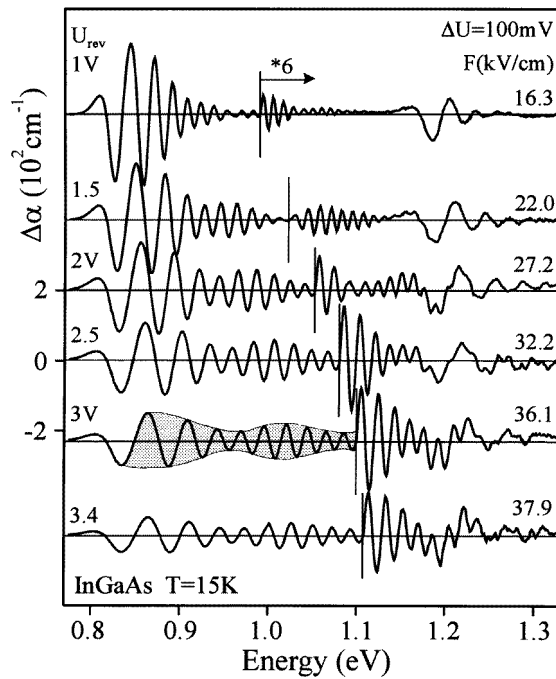


**Figure 2.** The variation of Franz-Keldysh oscillations with reverse bias. Different sets develop for the various valence bands showing the beat of light- and heavy-hole series (the shaded area). The weaker oscillations at higher energy have been amplified as indicated.

## 2. Experimental results

### 2.1. Comparison of absorption and electroabsorption spectra

The experiments were performed at low temperature on InGaAs crystals  $0.6 \mu\text{m}$  thick, grown by MOCVD, lattice matched to the n-InP substrate. The sample, capped with 50 nm of undoped InP, was sufficiently transparent up to the gap of InP to allow us to study field-induced changes of the transmission. Such electroabsorption spectra provide more direct access to modifications of the transition probability than electroreflectance spectra whose lineshape is strongly influenced by changes of the refractive index. Working with transmitted light also diminishes the influence of the inhomogeneous field near the surface. The field in the sample was altered by a dc bias applied between a thin (6 nm) semitransparent Pt contact on top and a grounded substrate. A much smaller ac voltage (square shaped) was used to monitor the influence of small fields on the spectrum as described before [16].

Figure 1 compares absorption and electroabsorption spectra for different bias voltages. Excitonic fine structure of the absorption spectrum appears if the built-in field is reduced by applying a forward bias. Slight tensile strain in the sample causes splitting of the light- and heavy-hole excitons by 5.7 meV. The narrow features of the electroabsorption spectrum,  $\Delta\alpha$ , under forward bias, result from field broadening of excitons with larger sensitivity of the light-hole exciton, as expected from its smaller binding energy and larger radius [17]. The field is too small for us to observe the response of the continuum states. A larger field of reverse bias ionizes the excitons, and the strain-induced fine structure disappears

from the spectra. The excitonic electroabsorption spectrum is replaced by the response of continuum states whose pronounced Franz–Keldysh oscillations reach far beyond the gap  $E_g$  [18]. In this range of fields, Coulomb interaction becomes negligible and the spectrum is well described by one-electron theory and the interband reduced mass  $m^*$ . The scaling of the spectrum with the electro-optic energy  $\hbar\Theta$  leads to a simple relationship of the peak position  $E_n$  and peak number  $n$ :

$$(E_n - E_g)^{3/2} = \frac{3ehF}{8\sqrt{2m^*}}(n + \varphi) \quad (3)$$

where  $\varphi$  varies little with energy and approaches 0.5 asymptotically [7]. This relation yields an electric field of  $11.5 \text{ kV cm}^{-1}$  for  $0.5 \text{ V}$  reverse bias based on effective masses of  $0.041m_0$  and  $0.45m_0$  for electrons and heavy holes, which dominate the  $\Delta\alpha$ -spectrum [18]. Under reverse bias the absorption spectrum shows a long absorption tail ending in a broad peak. Although this peak resembles a strongly broadened exciton it is not related to Coulomb enhancement but is the first positive peak of the Franz–Keldysh oscillations above the gap, which shifts with further increasing field to higher energy. The range of energy over which these oscillations can be observed contains the information on the coherence of band states.

## 2.2. Franz–Keldysh oscillations

An impressive series of oscillations develops in the electroabsorption spectra under increasing reverse bias as shown in figure 2. Although numerous Franz–Keldysh oscillations have also been observed in electreflectance spectra—particularly those of Ge [19, 20] and GaAs [21] near flat-band conditions—and by photoreflectance [22], such a large number at relatively small fields is exceptional and is attributed to the homogeneous field within the sample and, as will be shown, to the experimental procedure of switching between two fields of comparable strength. The series emerging at the fundamental gap passes at higher fields the transition energy of the split-off valence band at  $1.174 \text{ eV}$  where another set of Franz–Keldysh oscillations develops. The difference between the scaling energies  $\hbar\Theta$  of light- and heavy-hole transitions due to their different reduced masses leads to two sets of oscillations starting at the gap. Their superposition is responsible for the clearly visible beat in the spectrum, which has been noticed before in spectra of Ge and GaAs. Fourier transformation of the oscillations confirms the expected ratio ( $\sim 1.6$ ) of the reduced masses and a ratio of the amplitudes of about 3:1 which is consistent with the strength of heavy- and light-hole transitions. Detailed evaluation of this aspect will be published in a forthcoming paper. In this report we focus on the variation of the spectral range of the oscillations with increasing field.

More than 40 oscillations are observed and the peak positions obey equation (3) perfectly for Franz–Keldysh oscillations as shown in figure 3. Heavy-hole transitions determine the peak positions due to their larger oscillation strength while the contribution of light holes causes the small quasi periodic deviation of the data from straight lines. The field strengths derived from equation (3) increase for small bias linearly with bias voltage at a rate of  $11.5 \text{ kV cm}^{-1}$  for  $1 \text{ V}$  reverse bias, which is about  $3/4$  of the ratio of external voltage and sample thickness, a rate which decreases with increasing reverse bias. Part of the bias voltage is consumed by the variation of space charge in the contact regions and by the serial resistance. For the built-in field (zero bias voltage) due to the diffusion potential between the n-doped substrate and the Pt contact we find  $5.3 \text{ kV cm}^{-1}$  which corresponds to a diffusion potential of  $0.32 \text{ V}$ .

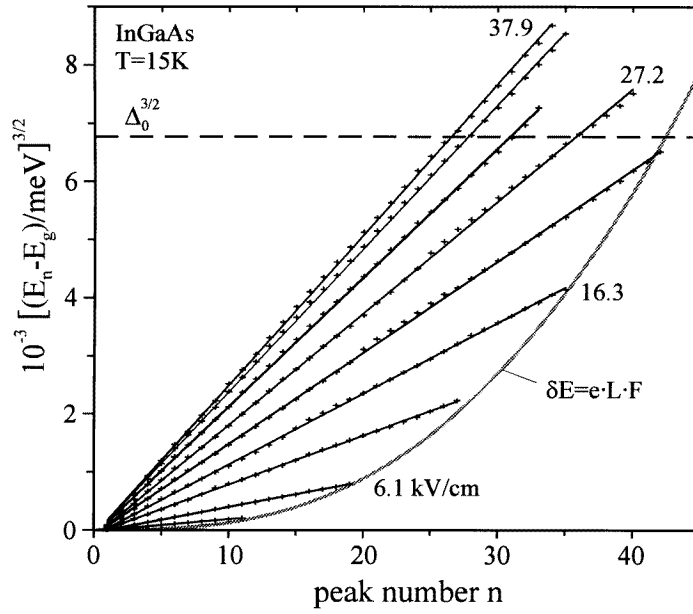


**Figure 3.** Peak positions  $E_n$  of Franz–Keldysh oscillations versus peak number  $n$  showing perfect agreement with theoretical prediction. The shaded boundary line corresponds to the observable range in the case of a field-independent coherence length of 160 nm.  $\Delta_0$  marks the energy gap of the split-off valence band.

### 3. Discussion

#### 3.1. The influence of inhomogeneous fields

Space charge not only consumes part of the external voltage but also causes some inhomogeneity of the field in the space charge region. We begin the discussion therefore with a qualitative consideration of the influence of space charge in the intrinsic region on the Franz–Keldysh effect. Observation of more than 40 oscillations seems to require a very homogeneous field in the sample to avoid destructive interference. In contrast to the case for electroreflectance where the surface field dominates, all regions contribute equally to the change of transmission which is the sum of all local changes  $\Delta\alpha(x)$  along the optical path:

$$-\frac{\Delta I}{I} = \int_0^d \Delta\alpha(x) dx = \int_0^d [\alpha\{F(x)\} - \alpha\{F=0\}] dx. \quad (4)$$

If the field were inhomogeneous, contributions from different parts of the sample would be out of phase due to a different electro-optic scaling energy  $\hbar\Theta$ , leading to rapid damping of the oscillations. However, the situation is different if we switch via a small voltage  $\Delta U$  from a field  $F_1(x)$  to another field  $F_2(x)$ . The change of transmittance caused by the modulation voltage  $\Delta U$  is now given as

$$\begin{aligned} -\frac{\Delta I}{I} &= \int_0^d [(\alpha\{F_2(x)\} - \alpha\{0\}) - (\alpha\{F_1(x)\} - \alpha\{0\})] dx \\ &= \int_0^d [\Delta\alpha\{F_2(x)\} - \Delta\alpha\{F_1(x)\}] dx \end{aligned} \quad (5)$$

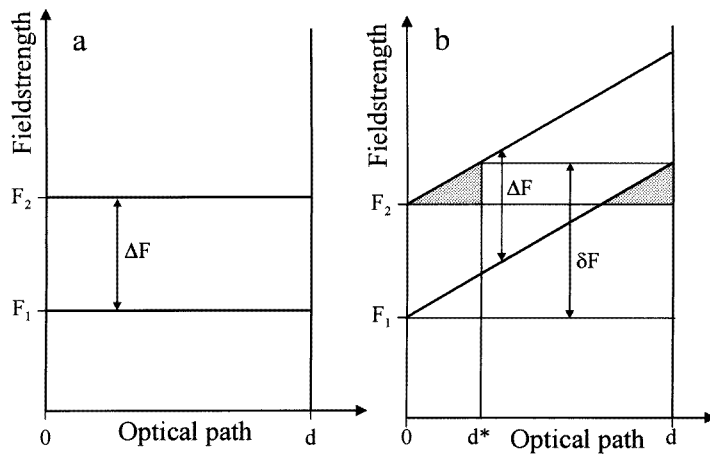


**Figure 4.** The scheme of the experimental situation for summing up field-induced absorption changes along the optical path of length  $d$  by switching from a field  $F_1$  to a larger field  $F_2$ : (a) without and (b) with a constant space charge. An inhomogeneous field of moderate strength  $\delta F$  has the effect of decreasing the effective optical path by  $d^*$  and increasing the modulating field. The two effects compensate for small modulation to produce the same change of transmittance as for a homogeneous field.

In the case of a constant space charge, maintained for instance by depleting residual dopants, the field will increase linearly across the sample up to an additional field  $\delta F$  as shown in figure 4(b). Switching the field from  $F_1$  to  $F_2$  by applying  $\Delta F$  leads for one part of the sample (between 0 and  $d^*$ ) to a field  $F_2$  which existed in the region between  $d - d^*$  and  $d$  before switching as field  $F_1$ . The high-field absorption on the left-hand side of the sample is the same as the low-field absorption on the other side, which modifies the resulting transmission change to

$$-\frac{\Delta I}{I} = \int_0^{d-d^*} [\Delta\alpha \{F_2(x+d^*)\} - \Delta\alpha \{F_1(x)\}] dx. \quad (6)$$

An inhomogeneous field  $\delta F$  thus leads to a reduction of the thickness by  $d^*$  along which field-induced changes contribute. The modulating field, on the other hand will be increased by the inhomogeneous field accumulated up to  $d^*$ , increasing the effective modulating field  $\Delta F$  by a factor  $d/(d-d^*)$ . Because the signal increases linearly for small modulation voltage, the resulting change of the transmittance is the same as in the case of a homogeneous field.

Equation (6) allows for a quantitative description of the measured electroabsorption spectra as shown in figure 5. The calculated curves were obtained by using the Airy functions as eigenstates of a free carrier in a constant electric field with a complex argument to account for spectral broadening [8]. The two experimental spectra were reproduced with the same set of material parameters, effective masses, absorption strength and broadening, changing only the fields. The fit yields the average field in the sample and the modulation field. The fields for the examples shown are sufficiently large that one can ignore excitonic effects. The bound states are broadened beyond recognition and the Coulomb enhancement of the absorption into their continuum is not altered by the small modulation voltage. The smaller modulation field at large reverse bias is consistent with the decrease of the rate by which the field increases with bias voltage. The modulation field of  $2.4 \text{ kV cm}^{-1}$  is

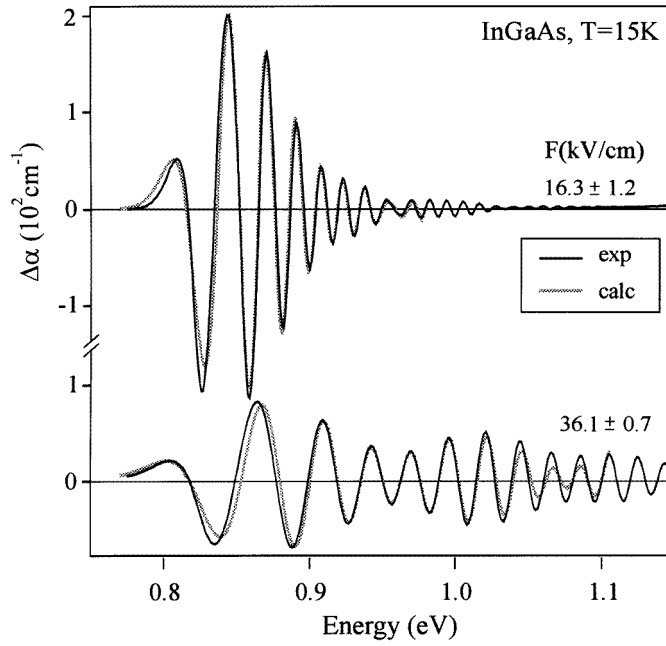


**Figure 5.** A comparison of electroabsorption spectra with small modulation of a static field with spectra calculated from Airy functions as eigenstates. A complex argument of the Airy functions was used to account for lifetime broadening. The fit yields the internal field and the modulation field which are the only parameters changed for the two spectra.

much less than the inhomogeneous field  $\delta F \approx 8 \text{ kV cm}^{-1}$  which would be accumulated across the sample if all residual dopants of an assumed concentration of  $10^{15} \text{ cm}^{-3}$  were depleted. Such a large modulation field would lead to a distinctly different shape of the electroabsorption spectra with beats between low- and high-field electroabsorption spectra. A detailed analysis which is beyond the scope of this report indicates an inhomogeneous field  $\delta F$  which is smaller than the modulating field of about  $2 \text{ kV cm}^{-1}$ . Space charges therefore are present only in a small part of the sample, which is consistent also with the appearance of discrete exciton states and sharp absorption edges under forward bias (figure 1). The diffusion potential therefore results mostly from electrons migrating from the n-InP substrate to the Pt contact and not from space charge within the sample.

### 3.2. The coherence length of band states

According to equation (1) the maximum momentum  $\delta k$  of accelerated carriers increases with field and scattering time  $\tau$ . If the scattering rate is independent of the field, the maximum value  $\delta E$  of the acquired kinetic energy increases quadratically with the field:

$$\delta E = \frac{(e\tau)^2}{2m^*} F^2. \quad (7)$$

Optical absorption should be altered over the same energy range because it contains the  $k$ -states which are mixed by the field to a new coherent excited state. For comparison with the experiment we define  $\delta E$  as the energy separation of the last clearly resolved Franz–Keldysh oscillation from the respective gap. Although this definition depends somewhat on



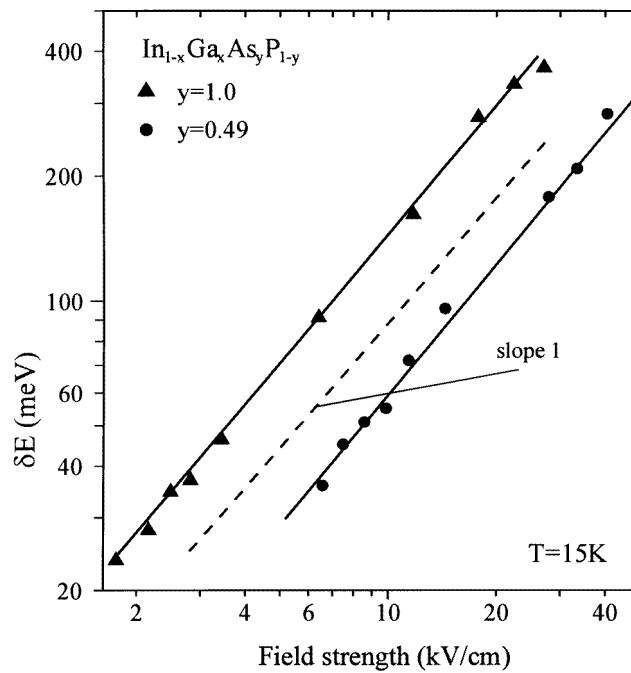


**Figure 6.** The linear increase with field of the range  $\delta E$  of Franz-Keldysh oscillations for the lattice-matched samples  $\text{In}_{1-x}\text{Ga}_x\text{As}_y\text{P}_{1-y}$ . The ternary sample shows the largest range, which corresponds to a coherence length of 160 nm.

the noise level and—very weakly—on the small modulation voltage, it should reveal the correct dependence of  $\delta E$  on the field  $F$  in the sample which is set by the much larger bias voltage. Figure 6 shows the variation of  $\delta E$  with field strength for the ternary sample in comparison with the behaviour of a quaternary sample. For fields above  $40 \text{ kV cm}^{-1}$ , Franz-Keldysh oscillations reach the absorption edge of the InP substrate,  $0.6 \text{ eV}$  above the gap. In order to avoid perturbation by the Franz-Keldysh oscillations of the split-off valence band, we consider only fields up to  $20 \text{ kV cm}^{-1}$  where the range of oscillations  $\delta E$  remains below the spin-orbit splitting  $\Delta_0$  of  $365 \text{ meV}$ . We find that over almost  $400 \text{ meV}$ , the range of Franz-Keldysh oscillations increases linearly with the field and not quadratically as expected from equation (7) which was based on a constant scattering rate, independent of the field.

The linear relationship of the field and range of Franz-Keldysh oscillations is not surprising if we recall that our experiment with high spectral resolution measures transitions between eigenstates and not the time evolution of wavepackets. Due to the electric field the  $k$ -vector is no longer a quantum number and the momentum space is not the appropriate space for representing the electron states. We prefer therefore to view the states in real space as shown in figure 7 which displays the wavefunctions of electron-hole pairs excited at  $z_0$  with the hole as reference and an electron of reduced mass  $m^*$  in the excited state. The shaded region shows the gap between the band edges which are tilted in the field. The excited state is the Airy function, the eigenfunction of a particle in a constant field [23]. The wavefunction is bound to the right by the external potential but not restricted to the left if scattering is absent. In a homogeneous medium identical excited states exist

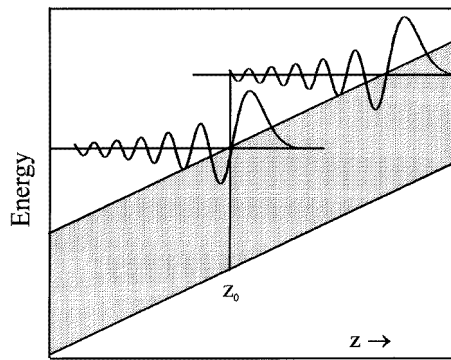


**Figure 7.** The energy diagram and excited states in real space for a homogeneous electric field. The shaded area shows the gap between the valence and the conduction band. Different excitation energies correspond to different locations of the excited states with respect to the ground state at  $z_0$ .

everywhere, but due to the electric field their energy differs by  $eF(z - z_0)$  from that of a state bound at  $z_0$  where the hole is located. Different photon energies excite states which differ only by their position  $z$  in the external potential. The situation is very similar to that of the Wannier–Stark transitions in a superlattice. However, the lattice constant  $a$  of the superlattice cell reduces the infinite number of excited states of the homogeneous medium to a finite number of states separated in space by integer multiples of  $a$  and in energy by  $eFa$ . Nevertheless, the number of observable Stark ladder transitions and the observable range of Franz–Keldysh oscillations depend in very much the same way on the coherence length of the electron states.

A coherent free-particle state has a finite coherence length  $L$  equivalent to its finite lifetime. Because only transitions into coherent states are modified by the field, the electro-absorption spectrum results from those excited states which spatially overlap with the hole at  $z_0$ , while more distant states do not contribute. If the coherence length is independent of the field the range of Franz–Keldysh oscillations increases linearly with field, in accordance with the experimental result, and is proportional to the coherence length:

$$\delta E = eLF. \quad (8)$$

Evaluation based on figure 6 yields for the ternary sample a coherence length of 160 nm and a smaller value of 60 nm for the quaternary sample of a composition in the vicinity of the miscibility gap of LPE samples. These values reduce by about a factor of 2 at room temperature. The observed linear relationship of  $\delta E$  and the field indicates that the coherence length of band states is independent of the field, as anticipated for the still moderate field strength.

If we equate the coherence length of an excited state, probed with high spectral resolution, with the mean free path of an electron, excited by a short spectrally broad pulse, typical fields in a diode of  $20 \text{ kV cm}^{-1}$  accelerate electrons of mass  $0.04m_0$  within 200 fs to an energy of 300 meV. This time is in the range of ballistic transport measured by emission of terahertz radiation [24], and even longer times are expected at smaller fields because of the field-independent coherence length. A mean free path independent of the field results if the scattering rate is proportionally to the drift velocity which is much larger than the thermal velocity. The calculation which reproduces the experimental spectra in

figure 5 so well used lifetime broadening of the Franz–Keldysh oscillations by a collision rate which increased proportionally to the drift velocity. It has been observed before that an energy-dependent lifetime describes damping of the Franz–Keldysh oscillations better than an energy-independent lifetime [25].

#### 4. Conclusion

In summary we have shown that Franz–Keldysh oscillations in a homogeneous field provide access to the coherence length of band states in semiconductors—a fairly unknown quantity which is difficult to measure. The Franz–Keldysh oscillations measure the coherence length of the excited electron–hole pair limited by scattering of either the electron or the hole. The oscillations are much better resolved if a small modulation voltage is used to increase an existing field in the sample, because this reduces the broadening of the spectra by space-charge-related field inhomogeneities. The method resembles photomodulation where screening by excited carriers modifies an internal field. However, due to an inhomogeneous distribution of photoexcited carriers, photomodulation leads to a spatially inhomogeneous modulation of the internal field. Although the range of Franz–Keldysh oscillations depends somewhat on experimental conditions, it serves well for defining and comparing the coherence lengths in different samples. The length is independent of the field but varies with sample quality, similarly to the exciton linewidth at low temperature and field [26]. This may change when oscillations from the fundamental gap reach the next gap, because then degenerate states belonging to different gaps begin to overlap spatially. The constant coherence length suggests for moderate fields that the coherent lifetime of an electron depends on the field, resulting in a field-independent mean free path. For fields exceeding  $40 \text{ kV cm}^{-1}$ , Franz–Keldysh oscillations cover more than 0.6 eV, pointing to coherent acceleration to large  $k$ -values but still not sufficient to reach the edge of the Brillouin zone and to allow observation of Wannier–Stark localization in bulk material.

The coherence length derived from the Franz–Keldysh effect is almost twice as large as the value derived from the photocurrent spectra of superlattices in the regime of Stark localization [1, 2]. This difference suggests either a superior material quality of our samples or—more likely—that the barriers in a superlattice provide additional scattering centres which reduce the coherence considerably below the coherence in bulk material.

#### References

- [1] Mendez E E, Agullo-Rueda F and Hong J M 1990 *Appl. Phys. Lett.* **56** 2545
- [2] Campi D, Cacciatore C, Neitzert H-C, Rigo C and Coriasso C 1993 *Superlatt. Microstruct.* **14** 253
- [3] Franz W 1958 *Z. Naturf. a* **13** 484
- [4] Keldysh L V 1958 *Zh. Eksp. Teor. Fiz.* **34** 1138 (Engl. Transl. 1958 *Sov. Phys.–JETP* **7** 788)
- [5] Callaway J 1963 *Phys. Rev.* **130** 549
- [6] Tharmalingam K 1963 *Phys. Rev.* **130** 2204
- [7] Callaway J 1964 *Phys. Rev. A* **134** 998
- [8] Aspnes D E 1967 *Phys. Rev.* **153** 972
- [9] Houston W V 1940 *Phys. Rev.* **57** 184
- [10] Wannier G H 1960 *Phys. Rev.* **117** 432
- [11] Bloch F 1928 *Z. Phys.* **52** 555
- [12] Bleuse J, Bastard G and Voisin P 1988 *Phys. Rev. Lett.* **60** 220
- [13] Leo K, Shah J, Göbel E O, Damen T C, Schmitt-Rink S, Schäfer W and Köhler K 1991 *Phys. Rev. Lett.* **66** 201
- [14] Feldmann J, Leo K, Shah J, Miller D A B, Cunningham J E, Meier T, von Plessen G, Schulze A, Thomas P and Schmitt-Rink S 1992 *Phys. Rev. B* **46** 7252

- [15] Aspnes D E and Studna A A 1973 *Phys. Rev. B* **7** 4605
- [16] Satzke K, Weiser G, Stolz W and Ploog K 1991 *Phys. Rev. B* **43** 2263
- [17] Blossy D F 1970 *Phys. Rev. B* **2** 3976
- [18] Weihofen R and Weiser G 1993 *Phys. Status Solidi b* **179** 563
- [19] Handler P, Jasperson S and Koeppen S 1969 *Phys. Rev. Lett.* **23** 1387
- [20] Ovsyuk N N and Sinyukov M P 1978 *Zh. Eksp. Teor. Fiz.* **75** 1075 (Engl. Transl. 1978 *Sov. Phys.-JETP* **48** 542)
- [21] Yin Y, Yan D, Pollak F H, Pettit G D and Woodall J M 1991 *Phys. Rev. B* **43** 12 138
- [22] Sydor M, Engholm J R, Dale D A and Fergestad T J 1994 *Phys. Rev. B* **49** 7306
- [23] Landau L D and Lifshitz E M 1959 *Quantum Mechanics* (New York: Pergamon) p 170
- [24] Hu B B, DeSouza E A, Knox W H, Cunningham J E and Nuss M C 1994 *Proc. 7th LEOS Conf. (Boston, MA, 1994)* vol 2, p 182
- [25] Satzke K, Weiser G, Höger R and Thulke W 1988 *J. Appl. Phys.* **63** 5485
- [26] Jaeger A, Weiser G, Wiedemann P, Gyuro I and Zielinski E 1995 *IEEE J. Selected Topics Quantum Electron.* **1** 1113